Electronic supplementary Information

Sequential on-off-on detection of Fe^{2+} and enantiomeric L-lysine with logic gate operation based on carbon dots derived from zinc-amine complexe

Xinlei Zhang, Peng Liu, Yuchi Zhang, Bohan Li, Yan Xu*

Department of Chemistry, College of Sciences, Northeastern University, Shenyang, Liaoning 110819, China.

***Corresponding Author:**

xuyan@mail.neu.edu.cn (Yan Xu)

Cell imaging

The viability of HeLa cells was determined by a standard methyl thiazolium tetrazolium (MTT) assay. Briefly, cells (5000 cells per well) were inoculated into each well of a 96-well culture dish and cultured in 100 mL DMEM at 37°C in 5% CO_2. After culturing the cells for 24 h, different concentrations of Zn-CDs were added to the cells and incubated for another 24 h. Cells were washed three times with PBS to remove excess carbon spots, MTT reagent in PBS (20 mL, 5 mg mL^{-1}) was added to each well and incubated for another 4 h at 37 °C. Finally, the formed purple crystals were dissolved in DMSO (150 mL) for 20 min at room temperature. The absorbance of each well at 490 nm was measured using a microplate reader.

HeLa cells were placed on culture dishes and incubated overnight in DMEM equipped with 10% fetal bovine serum in an air atmosphere containing 5% CO_2. Zn-CDs (100 μg/mL) were added to the culture dishes and the cells were incubated at 37 ºC. After 20 min, the mixed medium was removed and the cells were washed three times with PBS buffer (pH = 7). Images were captured using laser scanning confocal microscopy (LSCM). Then, the above cells were incubated with Fe^{2+} (100 μM) in a Petri dish for another 20 min, followed by the addition of L-Lys/D-Lys (200 μM) for 15 min. These images were taken by LSCM.

Temperature sensing related calculations

Absolute sensitivity (S_a) and relative sensitivity (S_r) are two important parameters in evaluating the temperature-sensing behaviors of optical thermometers. The S_a and S_r can be calculated from the following equations (1-2):

$$S_a = \left|\frac{\partial \Delta}{\partial T}\right| \qquad \text{* MERGEFORMAT (1)}$$

$$S_r = \left|\frac{S_a}{\Delta}\right| \qquad \text{* MERGEFORMAT (2)}$$

where Δ is used to represent the PL intensity ratio $I_{423\ nm}/ I_0$, and T is the temperature. Additionally, the temperature resolution (δT) is another key parameter for evaluating the sensitivity of optical thermometers for practical applications, which can be calculated according to the following equation (3):

$$\delta T = \frac{1}{S_r}\frac{\partial \Delta}{\Delta} \qquad \text{* MERGEFORMAT (3)}$$

in which the signal-to-noise ratio of the fluorescence spectrometer used is 16000:1, that is to say, the value of δΔ/Δ is about 0.0125% (Cao et al. 2021).

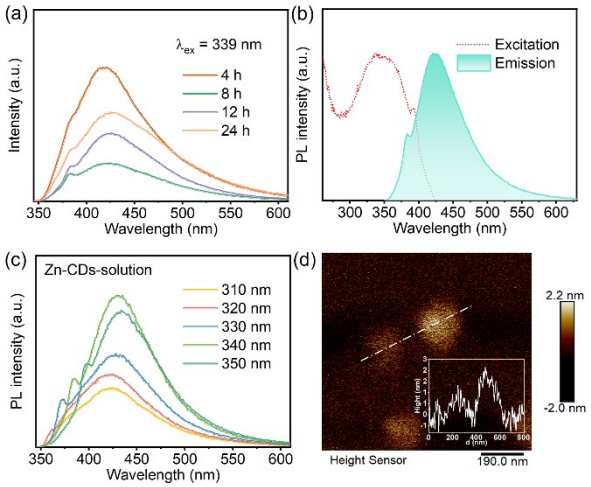

Fig. S1. (a) PL spectra of Zn-CDs (1 mg mL^{-1}) prepared from different hydrothermal reaction times; (b) Photoluminescent excitation (PLE) and emission spectra of Zn-CDs; (c) PL emission spectra of Zn-CDs aqueous solution under different excitation wavelengths; (d) AFM image and height profile of Zn-CDs.

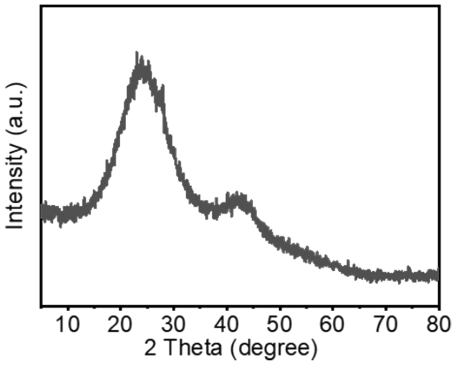

Fig. S2. X-ray diffraction pattern of Zn- CDs.

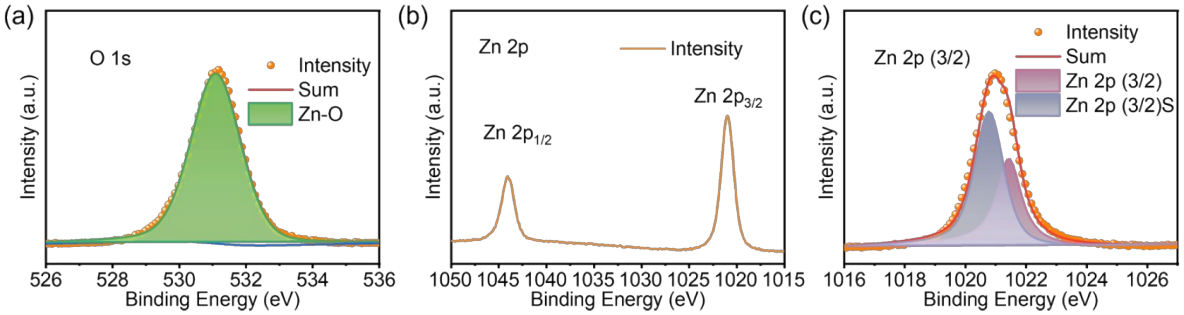

Fig. S3. XPS spectra of Zn-CDs (a) O 1s (b) Zn 2p and (c) Zn 2p (3/2).

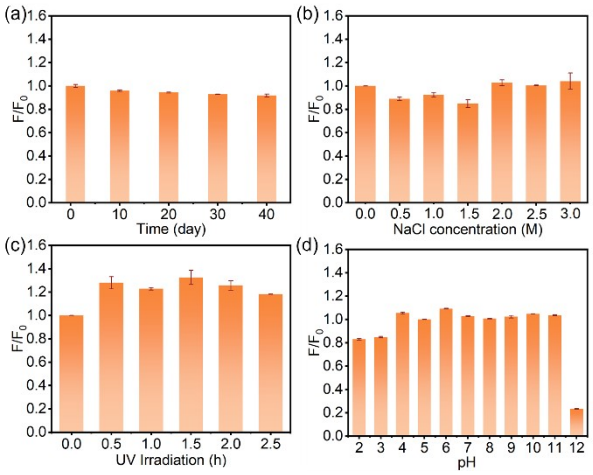

Fig. S4. PL intensity variation of F/F_o (F and Fo are the fluorescence intensity at ~423 nm with the presence and absence of different conditions, respectively) for Zn-CDs aqueous solution under different conditions of: (a) left time, (b) NaCl concentration, (c) UV irradiation hour, and (d) pH (λ_{ex} = 339 nm).

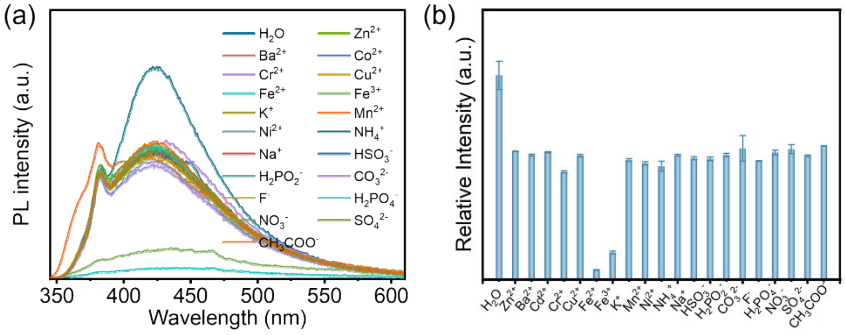

Fig. S5. (a) The PL emission spectra of 1 mM Zn-CDs in aqueous solution with the presence of various ions with a concentration of 1mM; (b) Effect of various ions on the PL emission intensity of Zn-CDs.

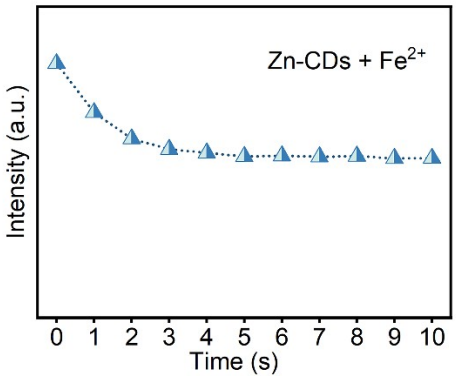

Fig. S6. Fluorescence response time of the sensor for Fe^{2+} detection. The fluorescence intensity was recorded at a wavelength of 423nm.

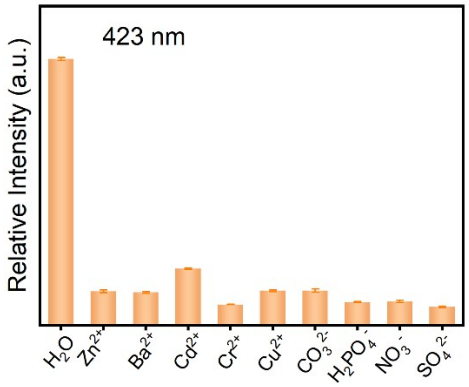

Fig. S7. The corresponding PL emission intensities of the Zn-CDs in pure H_2O and the other ions solutions (1 mM) after introducing 20 μL 3 mM of Fe^{2+} solution.

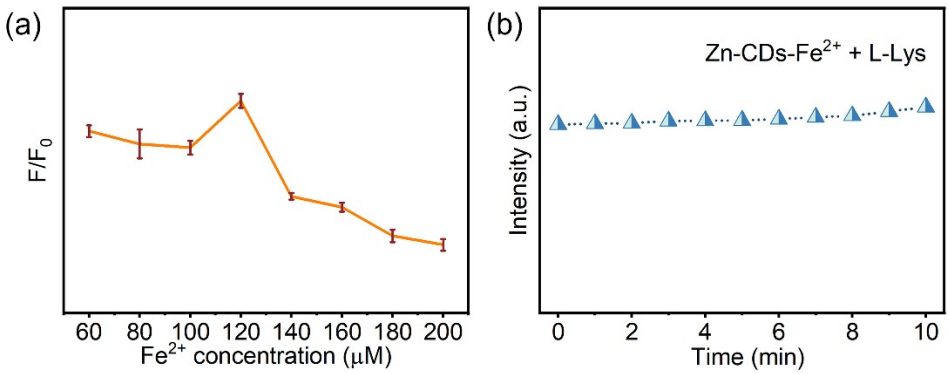

Fig. S8. (a) The influence of different concentrations of Fe^{2+} on the fluorescence intensity recovery of the Zn-CDs-Fe^{2+} system (the concentrations of the Zn-CDs and L-Lys were 1 mg/mL and 100 μM, respectively); (b) Fluorescence response time of the sensor for L-Lys detection. The fluorescence intensity was recorded at a wavelength of 423nm.

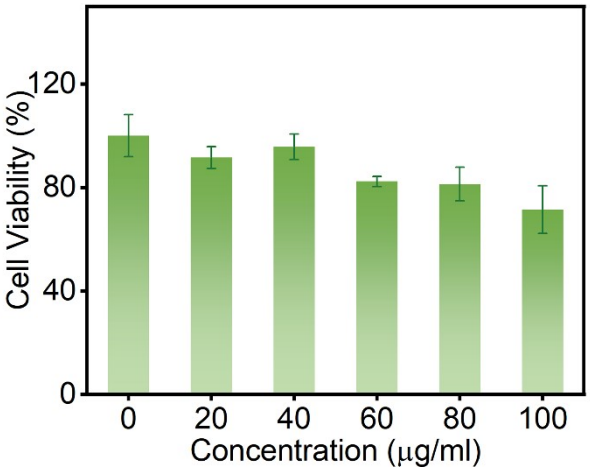

Fig. S9. Cell viabilities of Hela cells treated with Zn-CDs under various concentrations (0-100 μg mL^{-1}) for 24 h.

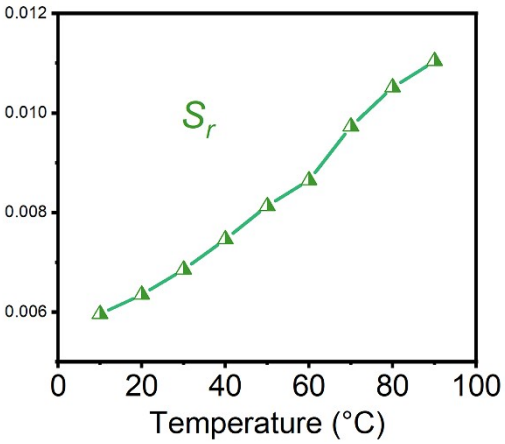

Fig. S10. Relative sensitivity of S_r versus temperature.

Table S1 Comparison of detection limits of various materials used for the detection of Fe^{2+}.

Materials[#]	Method	Linear range (μM)	LOD (μM)	Ref.
2HPN	Fluorescent	0−125	0.272	1
Cellulose-based sensor containing	Colorimetric	0-17.8	0.89	2
Carbon quantum dots (dopamine)	Fluorescent	0-50	0.038	3
Polyethyleneiminehydrochloride	Colorimetric	-	25.5	4
CDs (polyetherimide)	Fluorescent	0-500	0.051	5
Zn-CDs ($Zn(en)_3Cl_2$)	Fluorescent	0-120	0.092	This work

Note[#]: 2HPN = 2-((3-hydroxyphenyl)amino)-3-(phenylthio)naphthalene-1,4-dione

Table S2 Comparison of detection limits of different materials used for chiral L-Lys detection.

Materials[#]	Method	Linear range (μM)	LOD (μM)	Ref.
CQDs (ethylenediamine and L-cysteine)	Fluorescent	0-5000	970	6
MWCNT and TiO_2NPs	Electrochemical	0.5-5.5	0.39	7
CDs (neutral red and urea)	Fluorescent	0-700	0.019	8
CDs (citric acid and L-Asp)	Fluorescent	0-1000	3.34	9
CDs (Nigella sativa seeds)	Fluorescent	0-500	0.453	10
Zn-CDs ($Zn(en)_3Cl_2$)	Fluorescent	0-120	0.204	This work

Note[#]: CQDs = carbon quantum dots; CDs = carbon dots

Table S3. Comparison of the maximum relative sensitivity (S_r) of Zn-CDs with the other related optical thermometers reported previously.

Materials[#]	Sensitivity	Temperature range	Ref.
CDs&RB@ZIF-82-MMM	0.74% $^oC^{-1}$ (20 ^oC)	20-80 ^oC	[11]
Cys-CDs	0.64% $^oC^{-1}$ (70 ^oC)	10-70 ^oC	[12]
N, S-CDs	0.50% $^oC^{-1}$ (80 ^oC)	5-80 ^oC	[13]
CDs@UiO-66$(COOH)_2$-	0.82% $^oC^{-1}$ (10 ^oC)	10-80 ^oC	[14]
TbTATAB⊃C460	4.484% $^oC^{-1}$(27	-173-27 ^oC	[15]
Zn-CDs ($Zn(en)_3Cl_2$)	1.10% $^oC^{-1}$ (90 ^oC)	10-90 ^oC	This work

Note[#]: RB = rhodamine B; MMM = mixed-matrix membranes; ZIF-82 = zeolitic-imidazolate-framework-82; Cys = L-Cysteine; TbTATAB = terbium-based MOFB (H_3TATAB = 4,4',4''-*s*-triazine-1,3,5-triyltri-*p*-aminobenzoic acid); C460 = 7-diethylamino-4-methylcoumarin.

References

1. P. Ravichandiran, A. Boguszewska-Czubara, M. Masłyk, A. P. Bella, S. A. Subramaniyan, P. M. Johnson, K. S. Shim, H. G. Kim and D. J. Yoo, *ACS Sustain. Chem. Eng.*, 2019, **7**, 17210-17219.
2. H. Nawaz, W. Tian, J. Zhang, R. Jia, Z. Chen and J. Zhang, *ACS Appl. Mater. Interfaces*, 2018, **10**, 2114-2121.
3. M. Lu and L. Zhou, *Mater. Sci. Eng. C*, 2019, **101**, 352-359.
4. M. Yıldız, N. Demir, H. Ünver and N. Sahiner, *Sensor. Actuat. B-Chem.,* 2017, **252**, 55-61.
5. S. Wei, L. Tan, X. Yin, R. Wang, X. Shan, Q. Chen, T. Li, X. Zhang, C. Jiang and G. Sun, *Analyst*, 2020, **145**, 2357-2366.
6. F. Copur, N. Bekar, E. Zor, S. Alpaydin and H. Bingol, *Sens. Actuators, B* 2019, **279**, 305-312.
7. M. B. Gholivand, M. Shamsipur and N. Amini, *Electrochim. Acta,* 2014, **123**, 569-575.
8. D. Chang, Z. Zhao, H. Shi, J. Feng, Y. Yang and L. Shi, *Sens. Actuators, B* 2022, **362**, 131792.
9. P. Gao, Z. Xie and M. Zheng, *Sensor. Actuat. B-Chem.,* 2020, **319**, 128265.
10. N. Sharma and K. Yun, *Dyes Pigm* , 2020, **182**, 108640.
11. Y. Ding, Y. Lu, K. Yu, S. Wang, D. Zhao and B. Chen, *Adv. Opt. Mater.*, 2021, **9**, 2100945.
12. Z. Guo, J. Luo, Z. Zhu, Z. Sun, X. Zhang, Z.-c. Wu, F. Mo and A. Guan, *Dyes Pigm.* , 2020, **173**, 107952.
13. P. Zuo, J. Liu, H. Guo, C. Wang, H. Liu, Z. Zhang and Q. Liu, *Anal. Bioanal.Chem.*, 2019, **411**, 1647-1657.
14. X. Zhang, P. Liu, B. Li, X. Li and Y. Xu, *New J. Chem.*, 2022, **46**, 13021-13029.
15. T. Xia, T. Song, Y. Cui, Y. Yang and G. Qian, *Dalton Trans.*, 2016, **45**, 18689-18695.